



Recovering the line-of-sight magnetic field in the chromosphere from Ca II IR spectra

F. Wöger¹, S. Wedemeyer-Böhm², H. Uitenbroek¹, and T. Rimmele¹

¹ National Solar Observatory/Sacramento Peak, PO Box 62, Sunspot, NM 88349, USA
e-mail: fwoeger@nso.edu

² Institute of Theoretical Astrophysics, University of Oslo, Postboks 1029 Blindern, N-0315 Oslo, Norway

Abstract. We propose a method to derive the line-of-sight magnetic flux density from measurements in the chromospheric Ca II IR line at 854.2 nm. The method combines two well-understood techniques, the center-of-gravity and bisector method, in a single hybrid technique. The technique is tested with magneto-static simulations of a flux tube. We apply the method to observations with the Interferometric Bidimensional Spectrometer (IBIS) installed at the Dunn Solar Telescope of the NSO/SP to investigate the morphology of the lower chromosphere, with focus on the chromospheric counterparts to the underlying photospheric magnetic flux elements.

Key words. Polarization – Techniques: polarimetric – Sun: chromosphere – Sun: magnetic fields

1. Introduction

Advances in high-resolution observation techniques have yielded data suggesting the existence of a weak-field domain below the classical canopy (Wöger et al. 2006). Magnetic fields play a major role in the morphology of the chromosphere such as it is seen in the $H\alpha$ line core. The region below referred to as “fluctosphere” (Wedemeyer-Böhm & Wöger 2008) or “clapotisphere” (Rutten & Uitenbroek 1991) contains presumably only weak-fields. In numerical simulations, this domain is generated by interfering (acoustic) shock waves that are excited in the photosphere and propagate into the layers above (cf. Carlsson & Stein 1994).

Cauzzi et al. (2008) have shown that the Ca II infrared triplet provides a convenient and accessible diagnostic of the chromosphere. Confirming the shock behavior predicted by numerical models of radiation hydrodynamics in regions with no or only weak magnetic field, it has been found that there is a strong influence of magnetic field on acoustic processes such as shock signature suppression within that regime of the solar atmosphere (Judge et al. 2001; Vecchio et al. 2009). From these findings it has been concluded that this influence may be larger than generally expected, in particular because it is likely that there exist at least weak fields in this domain.

For this reason, knowledge of the chromospheric magnetic field topology and dynamics is of significant importance for the under-

Send offprint requests to: F. Wöger

standing of the solar atmosphere. Yet, these properties are poorly known due to limitations set by current observational techniques, in particular when gathering data of weak-field regions in the quiet Sun. In addition, the interpretation of chromospheric spectro-polarimetric data has proven to be difficult as many complicating effects have to be taken into account such as NLTE conditions.

Here we present and interpret high spatially resolved spectro-polarimetric measurements in the fluctosphere above strong photospheric magnetic features.

2. Model

A disadvantage of the robust center-of-gravity (COG) method (e.g., Uitenbroek 2003) to derive LOS magnetic flux is the lack of height resolution. To recover the height distribution of the magnetic flux, bisector analysis is often employed but it is more susceptible to noise. Thus, to enhance the reliability of a topology analysis, we suggest a technique that combines the bisector and COG methods.

2.1. The hybrid-COG method

The following steps are performed in our algorithm:

1. For both, the $I + V$ and $I - V$ spectra, find the two points (λ_a and λ_b) of intersection of the line profile with a horizontal line (the points at which the red and blue line wing have the same intensity).
2. Compute the COG of the $I + V$ and $I - V$ spectra (using the two acquired wavelength ranges) with

$$\lambda_+ = \frac{\int_{\lambda_a}^{\lambda_b} d\lambda \lambda \{(I + V)(\lambda_a) - (I + V)(\lambda)\}}{\int_{\lambda_a}^{\lambda_b} d\lambda \{(I + V)(\lambda_a) - (I + V)(\lambda)\}} \quad (1)$$

for $I + V$ and analogously λ_- for $I - V$.

3. Compute the value for the magnetic flux density along the line-of-sight: calculate the difference of the COG positions of the $I + V$ and $I - V$ profiles, using

$$B_{\text{LOS}} = \frac{\lambda_+ - \lambda_-}{2} \frac{4 \pi m c}{e g_L \lambda_0^2}, \quad (2)$$

where λ_0 is the central wavelength of the line, λ_{\pm} are the wavelength positions of the centroids of $I \pm V$, g_L is the effective Landé factor, and e and m are the electron charge and mass, respectively, in SI units (see Uitenbroek 2003, and references therein).

Step 1 allows to derive the magnetic flux density at different formation height ranges, as it is done in the genuine bisector approach. The even cuts are necessary to avoid bias in the measurement of the COG value. Obviously, the technique will work best for spectral lines without an emission peak, as it would make Step 1 (and Step 2) difficult by creating four instead of two points of intersection and also bias the computation of the COG. Asymmetries in the Stokes V profiles, such as those found, e.g., in a detailed analysis of a quiet-Sun region near network by Pietarila et al. (2007) on a common basis, pose a further problem. They can lead to biased measurements of magnetic flux. To test the proposed method, we have applied it to synthetic profiles that exhibit similar behavior.

2.2. Check of method

A magneto-hydrostatic model of a funnel-like expanding flux tube served as test case for the feasibility of our approach. The foot point of the flux tube in the deep photosphere has a diameter of 500 km and a magnetic field strength of 2 500 Gauss. For the Ca II IR line, synthetic NLTE spectra for all four Stokes parameters were computed. These served as input for the hybrid-COG method. The resulting output is compared to the initial flux tube model (Fig. 1).

The topology of the flux tube in the photosphere and chromosphere as well as the absolute magnetic flux density was recovered properly, and adjacent intensity levels show no significant jumps in the result thus exhibiting little noise. This is likely due to the inclusion of many points in the computation of the COG as opposed to the genuine bisector method. However, the three-dimensional topology in the higher layers cannot be directly interpreted because a bisector does not necessarily correspond to a thin atmospheric layer.

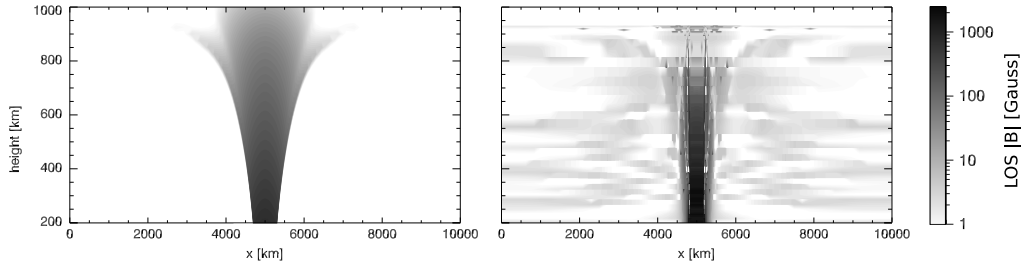


Fig. 1. Result of the accuracy test of the proposed hybrid bisector-COG method. Left: input model. Right: recovered flux density. The height scale for the recovered flux density was derived using calculations of $\tau_\lambda = 1$. The gray scale encodes the magnetic flux density and is the same for both panels.

To be able to compare our results with the model input, we computed the effective formation height for the Ca II infrared line by averaging the geometrical heights of the locations where $\tau_\lambda = 1$ over each of the wavelength intervals computed in Step 1.

The line formation height decreases from line core towards line wing and continuum. Furthermore, the formation height is affected by the presence of magnetic fields: due to the “Wilson effect” $\tau_\lambda = 1$ is different in magnetic and non-magnetic regions. As an example, compared to the ambient plasma the opacity within the model flux tube is lowered by the strong magnetic field. This leads to the formation of $\tau_\lambda = 1$ at a height that is about 200 km lower in the flux tube than in the non-magnetic atmosphere, which has been compensated for in Fig. 1 (right panel).

Comparing both panels of Fig. 1 allows us to test the reliability and estimate the error of the proposed technique. Line properties such as formation height and input parameters to technique such as the wavelength interval for Step 1 limit the recoverable height interval. The height distribution of the magnetic field of the modeled flux tube was recovered qualitatively. However, regions below the “canopy” of the flux tube show a weak signal in the reconstructed topology with strengths of up to (6 ± 1) G. Because of discontinuities in the magnetic field along the LOS, the Stokes V spectra show spikes and thus bias the $I + V$ and $I - V$ spectra. This leads to a fake magnetic signal in the reconstructed topology.

3. Data

In this section, we present observations of a quiet-Sun region located at disk center using the Ca II infrared line at 854.2 nm on 2008 September 22. Several persistent magnetic bright points are visible in the field of view, forming a network element (Fig. 2 a)–b).

In dual-beam spectro-polarimetric mode, the IBIS narrowband channel was configured to scan the Ca II IR line at 854.2 nm using six modulation states with exposures of 90 ms. An overall cadence of about 1 minute was achieved by sampling the line with 30 wavelength steps that were separated by 4.3 pm, where the full width at half maximum (FWHM) transmission of IBIS at this wavelength is 4.4 pm. The output data was a data cube with two spatial and one spectral dimension. Unfortunately, even after averaging 3 full scans after data reduction, the signal level of the Stokes Q and U component was below the noise level – no linear polarization was measured.

To gather context data about the magnetic field in the photosphere, a spectral region that includes both the Fe lines at 630.1 and 630.2 as well as the telluric blend separating these two lines was observed with a temporal offset of 1 minute. We have scanned the line with 30 wavelength steps with a stepwidth of 3.2 pm, where the FWHM of IBIS at this wavelength is 2.2 pm.

3.1. Data calibration

For the broadband images, the standard calibration method of dark- and gain-table correction was applied. In a subsequent step, the images were reconstructed with a speckle interferometric code adapted for use with high-order adaptive optics corrected data (Wöger et al. 2008). The reconstructed images were used in a later step to reduce atmospheric differential image motion in both the broad- and narrowband channels of IBIS.

As detailed in Cavallini (2006), the IBIS narrowband channel consists of two Fabry-Pérot interferometers, which are located in a collimated beam. This optical setup produces data that requires an elaborate procedure to take into account the blueshift in each pixel of a single narrowband exposure (Cavallini 2006). This procedure has been detailed by Janssen & Cauzzi (2006).

The calibration of the polarimetric data is accomplished with procedures originating from those of the Advanced Stokes Polarimeter (ASP; see e.g., Lites et al. 1993) adapted for the IBIS instrument. Residual crosstalk between the Stokes parameters has been removed manually. The quality of IBIS spectropolarimetric data has recently been compared with that of the spectrograph (SOT/SP) onboard the *Hinode* satellite. The result is that both instruments deliver very similar spectropolarimetric data, which indicates accurate calibration (Judge et al. 2009).

The adapted procedure to calibrate IBIS' spectroscopic and spectro-polarimetric data will be described in detail in a forthcoming publication (Tritschler et al. 2010).

3.2. Application of hybrid-COG

Analysis of our data set with the suggested hybrid method has been accomplished using 101 intensity values ranging from 18.5% (Ca II IR line core) to 32% of the local continuum intensity. To reduce salt and pepper noise introduced by the measured spectra, a median filter with 5×5 pixels (corresponding to $0''.85 \times 0''.85$) is applied to the data.

The COG method was applied to the Fe I line data to gather information about the underlying photospheric magnetic flux density which amounted to about 350 Gauss within the strongest feature. The small-scale magnetic elements were likely not resolved. The Fe I line is formed within a relatively thin atmospheric layer on the Sun, rendering the COG method sufficient, whereas the Ca II IR line has contributions from layers covering 1 000 km.

Hence the computed map of magnetic flux density is also a check for the values retrieved from the COG method using the Ca II IR line, which delivers a value of 250 Gauss using a cut at $\sim 50\%$ of the continuum intensity. As expected, the formation height at that level appears to be higher than that of the Fe I line.

Using the suggested hybrid method, starting at a level of 32% of the local continuum intensity, this value drops to 125 Gauss. This result is not surprising because a restriction of the method to the line core is equivalent to a restriction to higher layers. Further results of our hybrid bisector-COG analysis can be viewed in Fig. 2 d–f.

Two situations are of interest in the field of view. At location A in Fig. 2d, a patch of likely unresolved LOS magnetic flux disappears as when including only few points around the line core in the hybrid method, thus restricting the analysis to the highest layers. It appears as if the magnetic flux does not reach the corresponding heights. On the other hand, at the location marked B in Fig. 2d, a diffuse patch starts to show a filament structure at the high layers.

Overall, it appears that (i) the strong photospheric magnetic structure in the field of view fragments, and (ii) the flux density along the LOS, which corresponds to the vertical component of the field (the data were observed at disk center of the Sun), becomes smaller and weaker. A magnetic funnel expanding with height would show similar characteristics: the magnetic field becomes increasingly horizontal with height, and the vertical flux component decreases as the horizontal component, which is unfortunately currently not measurable with the IBIS instrument, increases.

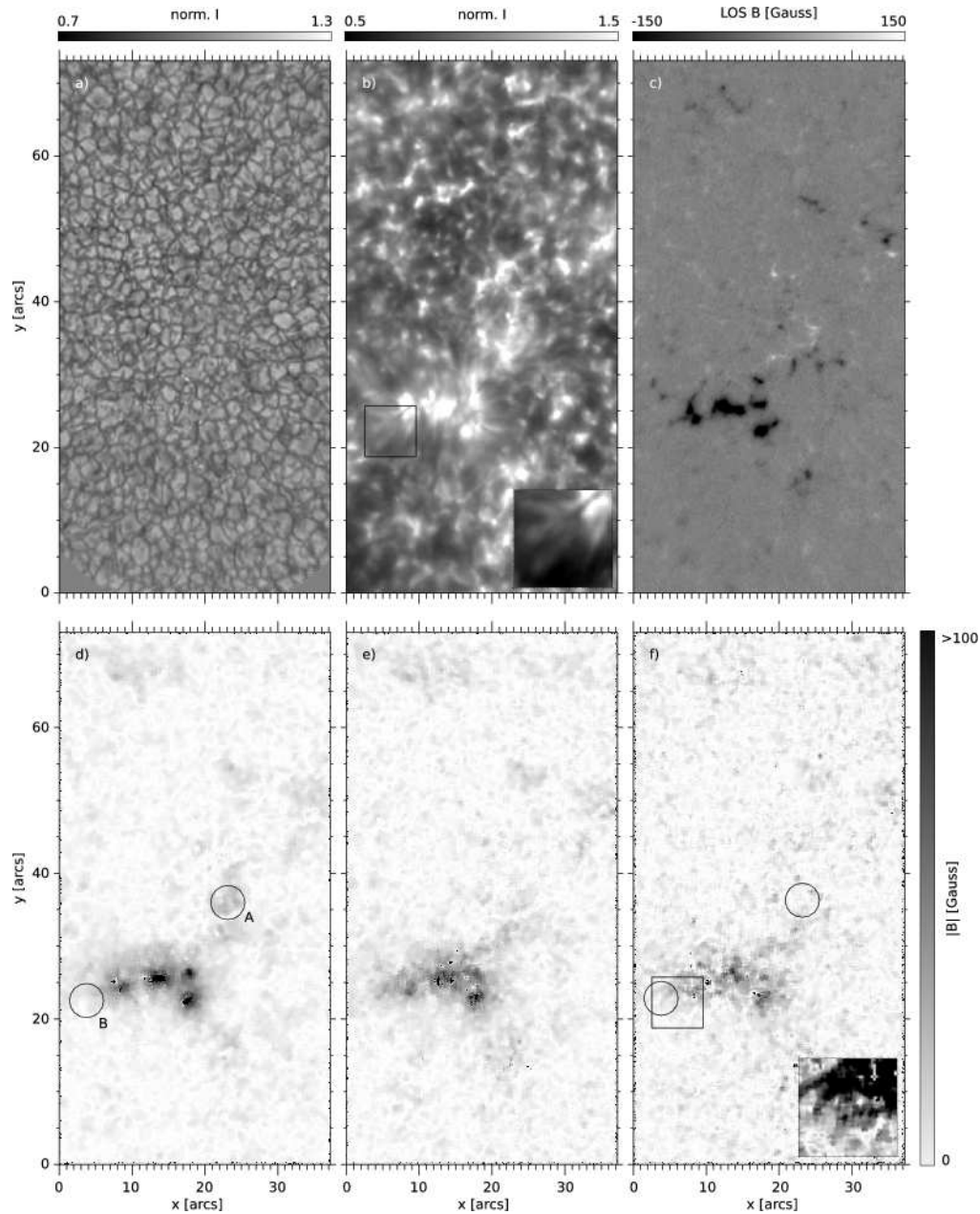


Fig. 2. a) Continuum intensity around 852 nm, b) Ca II IR (854.2 nm) line core intensity, c) LOS magnetogram computed from Fe I (630.2 nm). Cuts through the recovered 3D topology of the magnetic flux density by applying the hybrid bisector-COG method to the Ca II IR line scan. Panel d) is at 32% of the local continuum intensity (photospheric), e) at 20.2% and f) at 18.5% (chromospheric/“fluctospheric”). The subpanel in f) shows a contrast enhanced close-up of the fibrils marked by the box. At location A, a patch of magnetic flux along the line-of-sight seems to disappear with increasing height (also see subpanel). Location B is an example for the appearance of a filament like structure with height.

4. Conclusions

The focus of this contribution is the determination of the absolute LOS magnetic flux from spectro-polarimetric observations of the Fe I (630.2 nm) and Ca II IR (854.2 nm) lines.

We suggest to compute the 3D topology of the absolute LOS magnetic field flux per pixel using a new technique that is based on understood methods. The technique has been analyzed for accuracy for observations in a Ca II IR line in a quiet-Sun region near disk center. We were able to recover the topology of a strong magnetic structure extending from the photosphere to low chromosphere, and find that the magnetic flux becomes weaker with height developing a filament like structure as its height increases. The suggested method is not capable to infer filling factors. Thus, in an unresolved magnetic element, the field strength cannot be recovered.

While our findings suggest the existence of a funnel-like structure in the chromosphere, the location of the horizontal magnetic field remains unclear. Overall, we believe that a static flux tube funnel is a model too simplified to reflect realistically the conditions present in the chromosphere.

Understanding the chromospheric energy balance requires spatially highly resolved measurements of the magnetic field in the chromosphere. Such data, in spite of advanced instrumentation available at modern telescopes today, still lack the signal-to-noise ratio to gain the accuracy needed to detect weak fields at the temporal resolution which is implied by the variations seen in chromospheric diagnostics. The only way to address this problem is building a new generation of telescopes with larger apertures.

Interpretation of weak magnetic field measurements in the chromosphere is at least of equal difficulty as their detection or collection. New tools need to be developed to better understand the chromosphere as an important layer between the photosphere and corona; for example, the height in which the Stokes signals form are uncertain and do not only depend on specific contribution function used but also on the height distribution of the magnetic

field strength. Discontinuities and steep gradients in magnetic field strength remain to be fundamental problems: they are difficult to detect and to recover from measurements with methods available today.

Acknowledgements. SWB acknowledges support through a Marie Curie Intra-European Fellowship of the European Commission (6th Framework Programme, FP6-2005-Mobility-5, Proposal No. 042049). The authors would like to thank A. Tritschler for support during the data reduction. NSO is operated by the Association of Universities for Research in Astronomy, Inc. (AURA), for the National Science Foundation.

References

- Carlsson, M. & Stein, R. F. 1994, in *Chromospheric Dynamics*, ed. M. Carlsson, 47
- Cauzzi, G., Reardon, K. P., Uitenbroek, H., et al. 2008, *A&A*, 480, 515
- Cavallini, F. 2006, *Sol. Phys.*, 236, 415
- Janssen, K. & Cauzzi, G. 2006, *A&A*, 450, 365
- Judge, P., Tritschler, A., Uitenbroek, H., et al. 2009, *ApJ*, in press
- Judge, P. G., Tarbell, T. D., & Wilhelm, K. 2001, *ApJ*, 554, 424
- Lites, B. W., Elmore, D. F., Seagraves, P., & Skumanich, A. P. 1993, *ApJ*, 418, 928
- Pietarila, A., Socas-Navarro, H., & Bogdan, T. 2007, *ApJ*, 670, 885
- Rutten, R. J. & Uitenbroek, H. 1991, *Sol. Phys.*, 134, 15
- Tritschler, A., Reardon, K. P., Wöger, F., Tomczyk, S., & Casini, R. 2010, *ApJ*, in preparation
- Uitenbroek, H. 2003, *ApJ*, 592, 1225
- Vecchio, A., Cauzzi, G., & Reardon, K. P. 2009, *A&A*, 494, 269
- Wedemeyer-Böhm, S. & Wöger, F. 2008, in *Waves & Oscillations in the Solar Atmosphere: Heating and Magneto-Seismology*, ed. R. Erdélyi & C. A. Mendoza-Briceño, IAU Symp., 247, 66
- Wöger, F., von der Lühe, O., & Reardon, K. 2008, *A&A*, 488, 375
- Wöger, F., Wedemeyer-Böhm, S., Schmidt, W., & von der Lühe, O. 2006, *A&A*, 459, L9